International Journal of Agriculture and Environmental Research

ISSN: 2455-6939

Volume:05, Issue:01 "January-February 2019"

A NEW APPROACH TOWARDS A SMART MECHANICAL INTRA-ROW WEEDING

Paolo Liberati[a]*, Alberto Assirelli[b]

[a]Agricultural and Food Sciences Department - DISTAL,
University of Bologna - Viale G. Fanin 50, Bologna, Italy.

[b]Council for Agricultural Research and Economics (CREA) - Research Center for Engineering and Agro-Food Processing; Monterotondo, Rome, Italy.

*Corresponding author

ABSTRACT

Organic farming, in a modern context of precision agriculture, requires new tools in order to improve the quality and efficiency of field operations, while reducing their costs. This theoretical study will present and analyse new approaches to perform mechanical weeding inside the row in horticulture fields. The idea is to weed the row by skipping the crop by means of a rotating system instead of a traditional crosswise one. In this way the machine follows the direction of the working progression (although this is not possible for all the proposed models) thus avoiding the displacement of machine inertial mass orthogonally to the working trajectory, which tends to unbalance the machine, and increase fuel as well as components' consumption. The different configurations experimented by means of simulation models have shown different solutions: the horizontal axis rotating plant-skipping system (RPSS-HA) allows to work only within the row, while all the other models (with vertical rotating axis RPSS (RPSS-VA), the forward-backward tilting plant-skipping system on a vertical axis (FBTS), with constant or variable rotation speed, respectively FBTS-CR, and FBTS-VR) present also a worked area outside the row. This study highlights also the need of new approaches in the design of working tools, in order to substitute, for example, the traditional "heavy" working tools (blades, teeth, hoes, etc.) with lighter ones.

Keywords: mechanical weed control; precision control weeding; modeling; organic farming.

Abbreviations

RB = Rotating body (holding 2, 3 or 4 THFs)
THF = Tool holder frame

WT = Working Tool supported by the THF
RZ = respect zone; a circular area centred on the crop plant to be skipped by mechanical weeding
CDSS = Crosswise Displacement plant-skipping System
MWAR = Maximum Workable Area
RPSS = Rotary motion Plant-Skipping System

See Tab. 3 for the abbreviations of the operating working parameters.

Symbols

$D_{t\,min}$ = (m) minimum distance between plants in the row required to avoid plant damaging (RPSS-HA model)
X_R = (m) entering distance in CDSS model
n_{wt} = number of working tools, each mounted on a THF
r_r = (m) radius of the RZ
r_t = (m) radius of the working tool
v_a = (m s^{-1}) advancing velocity in CDSS model
v_r = (m s^{-1}) crosswise translation of the THF in CDSS model
α_{THF} = (rad) angle between two adjacent THFs
α_{min} = (rad) THF angular position to calculate the minimum distance between two plants in the row (RPSS-HA model)
ω_{rot} = (rad s^{-1}) minimum angular velocity of the THF to skip the plant
ω_{RcR} = (rad s^{-1}) return angular velocity in the row at constant speed rotation (FBTS-CR model)
ω_{RvR} = (rad s^{-1}) return angular velocity in the row at controlled speed rotation (FBTS-VR model)

1. INTRODUCTION

The cultivation of fruit trees and vegetable crops in open fields is becoming more and more important in the Italian agriculture. In the last few years, three important events have encouraged the development of alternative technologies to chemical weed control. First of all, the ascertained toxicity of products such as glyphosate (1); in Europe, some Commission implementing Regulations restrict its use that is monitored by the Committee on the Food Chain and Animal Health. Secondly, the high number of plants of commercial interest have developed resistance to active principles such as the glyphosate (Salas ET AL., 2012; Gaines et al., 2010; Perez-Jones ET AL. 2005); finally, the focus on a type of sustainable agriculture is causing many farmers to shift to organic farming.

ISSN: 2455-6939

Volume:05, Issue:01 "January-February 2019"

In Italy, the 6th General Census of Agriculture has allowed us to collect information on the structure of organic farms. In particular in our Country there are 44,455 organic farms (2.7% of the total). Their presence in the South is particularly significant, with 63% of the farms engaged in organic production; on the other hand, the islands recorded the widest biological surface average per farm (24.9 hectares) and the largest number of livestock farms converted to organic farming, for almost all bred species (source: ISTAT).

These farms are particularly important both because they contribute to the spread of forms of land and farm management in a compatible way with the protection of the environmental, soil and genetic diversity, and because it would foster the best quality of products. In general, the locution "Organic Farming" is a cultivation and breeding method that allows only the use of naturally occurring substances, while excluding the use of synthetic chemical substances (fertilizers, herbicides, insecticides). In this perspective it is evident how the use of mechanical or physical control systems (as an alternative to the normal practice of chemical weed control) becomes essential.

To limit weed problems, a series of preventive measures can be implemented through the choice of variety, planting rather than seeding, prevent seed production, choosing the field, preparing the seedbed, deciding the crop sequence, covering the soil, accurate seeding and planting, growth of the crop. Some of these have a moderate effect on the subsequent growth of weeds, but some others, such as planting rather than seeding, preparing the seedbed, deciding the crop sequence, covering the soil, accurate seeding and planting, growth of the crop, are operations which limit the development of weeds. The additional attention required by this approach will be recouped in the form of fewer time for weeding during the cultivation of the crop. Anyway, despite several years trying to work on the competitiveness of crops versus weeds (Hoad et al. 2008; Davies et al. 2004), their control still represents a very critical aspect, and not only for Italian agriculture.

To these preventive techniques need to be matched, during cultivation, to weed control practices, especially for the control of weeds which develop intra-row, and are not affected by inter-row cultivation, such as hoeing. Intra-row weeds, if insufficiently controlled, cause major problems for organic intra-row crops, such as vegetables and maize (Zea mays L.). Intra-row weeding is expensive, time consuming and difficult to plan, as shown in Tab. 1.

The control of weeding using a mechanical tool, e.g. with hoe and rotary tiller, is by far the most used technique during the first years of the plant. There is a wide variety of tools in the market, which can be more or less expensive and more or less effective to implement this operation along the row without damaging the young plants of the crop. The choice is guided by a prevention approach by applying better practices of fertilization and irrigation, although the direct

ISSN: 2455-6939

Volume:05, Issue:01 "January-February 2019"

intervention on weeds through mechanical, physical or biological methods is far more important (Tab. 2).

Table 1: Hours per hectare required for manual intra-row weeding in organic farm in Netherlands (Van der Weid et al., 2008).

Crop	Planting method	Labour (hours ha^{-1})
Onion	Sown	177
Carrot	Sown	152
Sugar beet	Sown	82
Sugar beet	Planted	28
Vegetables	Planted	46
Cereals	Sown	12
Potato	Sown	9

Especially in the field of mechanical systems, for many years weeding approach follows the same functional methods, although using different types of tools and variously articulated plant-skipping systems, dating back to the principles developed several decades ago, in the early '70s.

Table 2: Possible direct intervention techniques to control weeds.

Mechanical weeds control	Physical weeds control	Biological methods
Mowing	Flame wedding	Grassing controlled with specific herbs
Powered rotary weeder	Soil tillage	Appropriate crop rotation
Brush weeder	Preventive and cultural methods	Species and varietes competitive with weed
Rotary ground driven weeder	Solarisation	Cover crops
Harrow comb. weeder	Electromagnetic weed control	Intercropping techniques
Spring tine weeder	Steam wedding	Catch crops
Sweep hoe weeder	.....	.....

ISSN: 2455-6939

Volume:05, Issue:01 "January-February 2019"

As described in Peruzzi et al. (2017), and Van der Weide et al. (2008), simplified mechanical weeders (for example, cultivators) are mainly used in low-density crops, while in high-density crops spring harrows are used. Instead, Flame systems are suitable for all crops independently from seeding density. Among the simplified systems we can count spring-tine harrows and cultivators, and, among new techniques, finger-weeders and torsion-weeders. An interesting low-cost approach to weed a maize field is proposed by Rueda-Ayala et al. (2015) by controlling the tine angle of a harrow.

In literature there are several innovative systems to skip the crop plants. For example, Pérez-Ruíz et al. (2014) used two hoes in the close position to work intra-row, and opening them laterally like a scissor to skip the crop plants. A similar approach is used in the *Sarl Radis* model, as described in Van der Weide et al. (2008). Rasmussen et al. (2012), designed a rotor tine cultivator to skip the crop plant. A similar approach was used by Li et al. (2015) designing a controlled rotating blade (sickle-shaped).

With regard to the last two works, our study investigates systems to skip crop plants by adopting a rotating system.

Dimensions, shape and weight of the tools related to specific operating modes strongly characterize the different types of machines with respect to their working methods in field operation. From this point of view, the present work is intended to provide useful indications to combine the type of tool and working mode of the machine, its intra/inter-row working modality, and the possible development phase.

From this point of view, the present study, that gives a new approach to skip crop plants, can be linked to already available systems to weed without using mechanical tools. Among these we can mention, for example, the high-pressure water system and the well-known systems using free or guided flame by liquid propane. But there are also more sustainable recent systems, characterised by commercial success, such as that using wooden pellets for combustion, integrated or not with perimetrical jets of boiling water or steam to increase the herbicide effect, and, in the same time, to reduce the risk of fire in summer usage. Other hot foam systems are being tested at Italian research institutions.

All these systems, even though they do not use moving parts, cannot be turned off during their usage to save the crop plant (and turned on when needing to remove weeds), and cannot be turned off too rapidly, and therefore they need a mechanical crop plant-skipping system.

2. MATERIALS AND METHODS

ISSN: 2455-6939

Volume:05, Issue:01 "January-February 2019"

The model taken as a reference model in the present work is the traditional one which uses the displacement of the tool holder frame (THF, the body carrying the working tool) in the crosswise direction, with respect to the driving direction, to exit/enter from/in the row, to avoid contact with or damages of the plant. The proposed models, instead, use a THF rotating motion to exit/enter the row; the rotation may be continuous in the direction of advancing, or discontinuous, both in the advancing direction or in its opposite direction (to enter and exit the row); moreover, a tilting motion approach has been taken into consideration.

For all the proposed schemes numeric simulation models were developed, including the classical ones with the aim of evaluating in a comparative way the main processing indexes as a function of some operating parameters (operating speed, angular velocity of THF rotation, THF radius of rotation, etc.).

Although the models provide analytical solutions, some aspects of the simulation have been solved by means of a numerical approach, which was necessary to identify more easily the different kind of worked areas (Tab. 3 and Fig. 1). The developed code implements a map of the worked area by tracking the working tool (by simulating its rotation and translation).

The analytical solution was used to determine the necessary operating parameters for the correct operation of each machine (THF rotation and translation speed), trying to define the most salient aspects of each application solution.

Table 3: Calculated indexes for the characterization of the worked area (see Fig. 1).

Parameter	Definition
1. RWA	Row centered worked area (m^2)
1.1.RWA%	Percentage of 1.RWA in terms of 1.2.WCA (%)
1.2.WCA	Workable row centered strip area (m^2); the strip of soil as wide as the working tool (2 r_t) between two different plants, and centered in the row.
2. OWA	Outwards worked area (m^2); worked area outside RWA.
2.1.OWA%	Percentage of 2.OWA in terms of 5.OWBA (%).
2.2.OWAR%	Outwards worked area 2.OWA in terms of 1.RWA (%).
3. WWA	Width of the worked area (m) considered from the row towards the

ISSN: 2455-6939

Volume:05, Issue:01 "January-February 2019"

	enter/exit side of the THF.
4. WR	Worked row (excluded the respect zone) (m).
4.1.WR%	Percentage of the worked row 4.WR in terms of 6.WBR (%).
5. OWBA	Outwards workable area (m^2); its width depends on the selected model.
6. WBR	Workable row (plant spacing excluded the respect zone, r_r) = D/2 r_t.

For all the simulated models, a safety zone (respect zone, RZ) has been established in order to allow a comparison of the characteristics of the worked areas, represented by a circular surface, of radius r_r, centered on the plant. The operational processing parameters are calculated to work, as far as possible, the whole row excluding the safety zone (6.WBR).

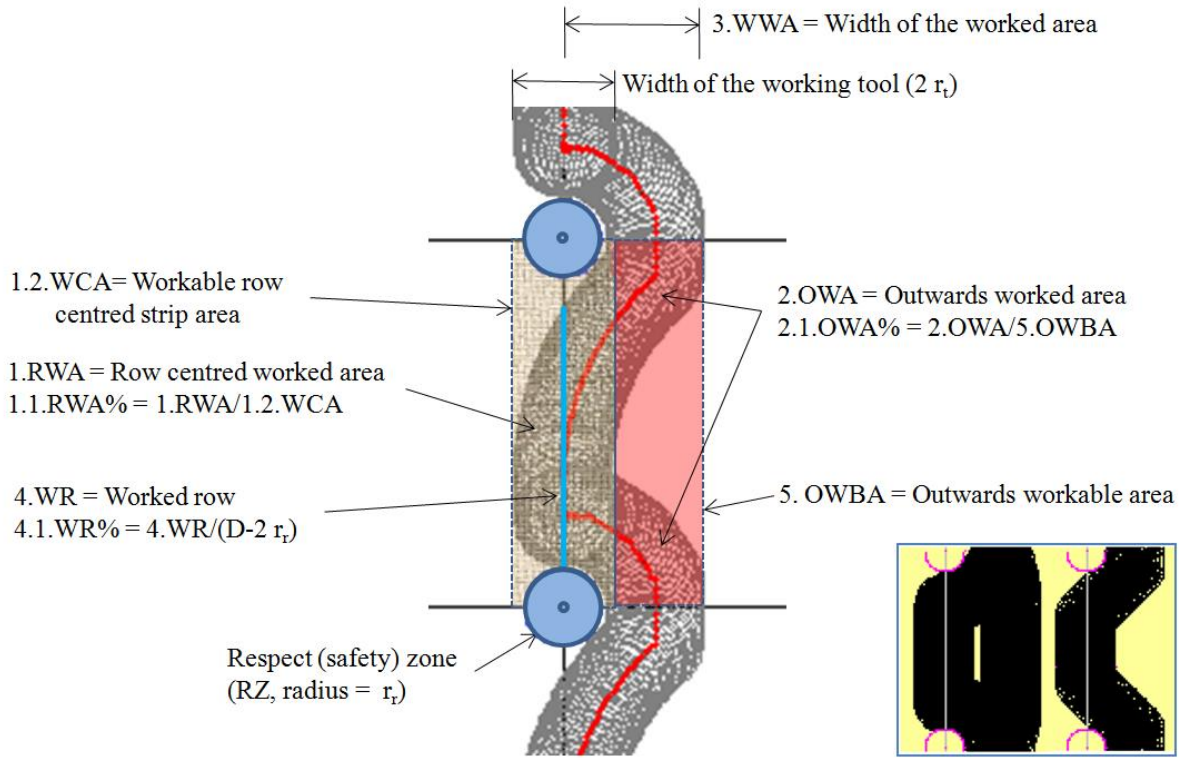

Figure 1: Operating parameters considered for the comparison among the simulated models. The gray track represents the worked area; circular areas represent the safety zones around the plants (RZ). In the box on the right the numerical mapping result from the RPSS-VA model with 2 THFs (left), and the CDSS model (right).

ISSN: 2455-6939

Volume:05, Issue:01 "January-February 2019"

Simulated models

The simulated models differ in how to skip the plant during the working of the row. The classic model skips the obstacle exiting the row by a crosswise displacement of the working tool (here called the Crosswise displacement plant-skipping system, CDSS). All the other proposed models, instead, use the rotation of the tool holder frame (THF) as plant-skipping system.

Finally, to make the simulation realistic, a vertical rotary spike-tooth harrow, of radius r_t, was used as exemplary working tool (WT). In fact, the WT may also be of another type, even lighter if possible, also newly designed, in order to meet the spirit of the present work, that is to create a light and simplified working system.

2.1. Crosswise displacement plant-skipping system (CDSS)

As already told, CDSS is the traditional model. The plant is skipped by a crosswise movement of the THF, with a motion perpendicular to the direction of the path.

Taking into account the RZ with radius r_r surrounding the plant, the point where the THF has to begin its exit from the row (X_R point in Fig. 2), in order to avoid trespassing the RZ, is calculated using the following formula:

$$X_R = X_F + r_t \qquad (1)$$

where:

$$X_F = -\frac{a_F}{b} \qquad (2)$$

$$a_F = \frac{r_r + r_t}{\cos(\alpha)} \qquad (3)$$

$$\alpha = atn(b) \qquad (4)$$

Where *b* is:

$$b = \frac{v_r}{v_a} \qquad (5)$$

ISSN: 2455-6939

Volume:05, Issue:01 "January-February 2019"

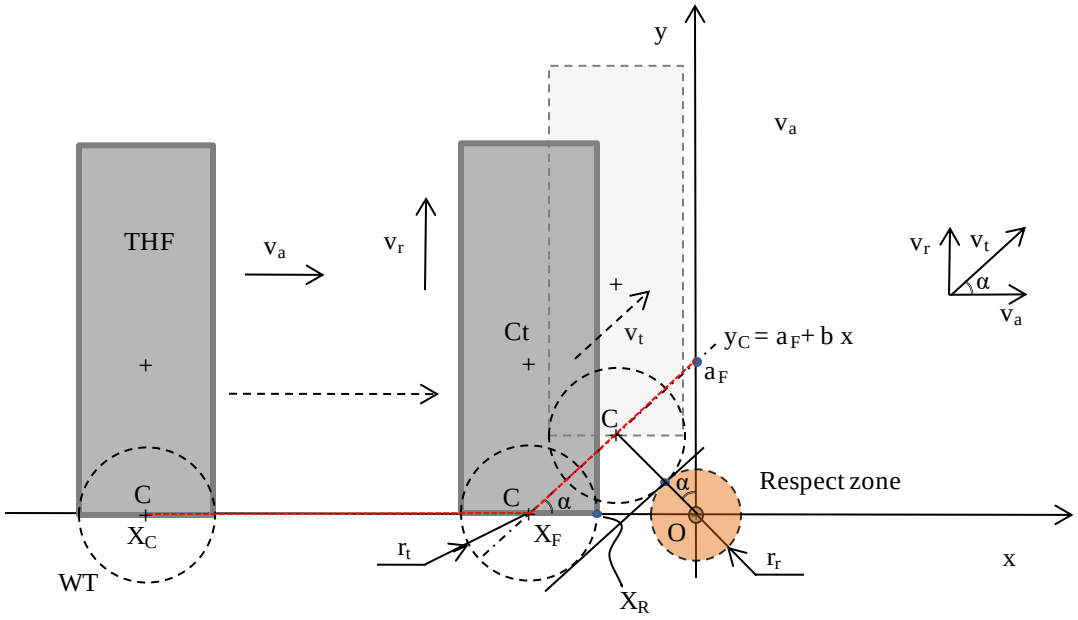

Figure 2: Sketch of the crosswise displacement plant-skipping system (CDSS).

The exit of the THF will continue until the lower point of the WT is out of the respect zone; considering the trajectory of the center C of the WT described by the equation $y_C = a_F + b\,x$, this condition is verified when $y_C = r_t + r_r$. So the exit will end when $X_C = (r_t + r_r - a_F)/\,b$. The row re-entering will follow a symmetrical direction.

2.2. Rotating tool holder frame - vertical rotation axis (VA)

2.2.1. Rotary motion plant-skipping system (RPSS-VA)

In this model there are two, three or four THFs radially arranged around the rotating body RB (Fig. 3); each THF is equipped with a WT (Fig. 3). When a THF is working in the row, it is perpendicular to the row itself and fixed (not rotating). When the plant is signaled by a suitable sensor system, the RB start a rotation at a proper velocity (ω_{rot}) in the opposite direction compared to the running one; this allows the THF to exit from the row to preserve the RZ. The rotation will end after an angle of π/n_{wt} rad (n_{wt} = number of working tools); at this point, the THF closer to the one that just left the row will be perpendicular to the row itself with its WT ready to work.

Calculation of the angular velocity (ω_{rot}) to skip the plant

ISSN: 2455-6939

Volume:05, Issue:01 "January-February 2019"

With reference to Fig. 3 it is possible to establish that the THF inside the row should begin its rotation just when its point A is against the RZ (at the distance of r_r from the plant). The rotation will end after an angle of π rad, when point B "touches" the RZ on the other side of the plant. In this context the travelled distance by the centre C_t of the rotating body (RB) during its rotation will be $2 \cdot (r_r + r_t)$, with a rotation time of $t_r = 2 \cdot (r_r + r_t)/v_a$. In general, considering n_{wt} as working tools (with n_{wt} = 2, 3 and 4, Fig. 3) the rotation angle of the THF needing to skip the plant is $\alpha_{THF} = 2\pi / n_{wt}$ (rad); consequently, the correct angular velocity ω_{rot} of the THF is given by the following equation:

$$\omega_{rot} = \frac{\alpha_{THF}}{t_r} = \frac{\pi \cdot v_a}{n_{WT} \cdot (r_r + r_t)} \qquad (6)$$

In this way the plant will be skipped without undergoing any damage and without invading the RZ. Higher n_{wt}, lower will be ω_{rot}.

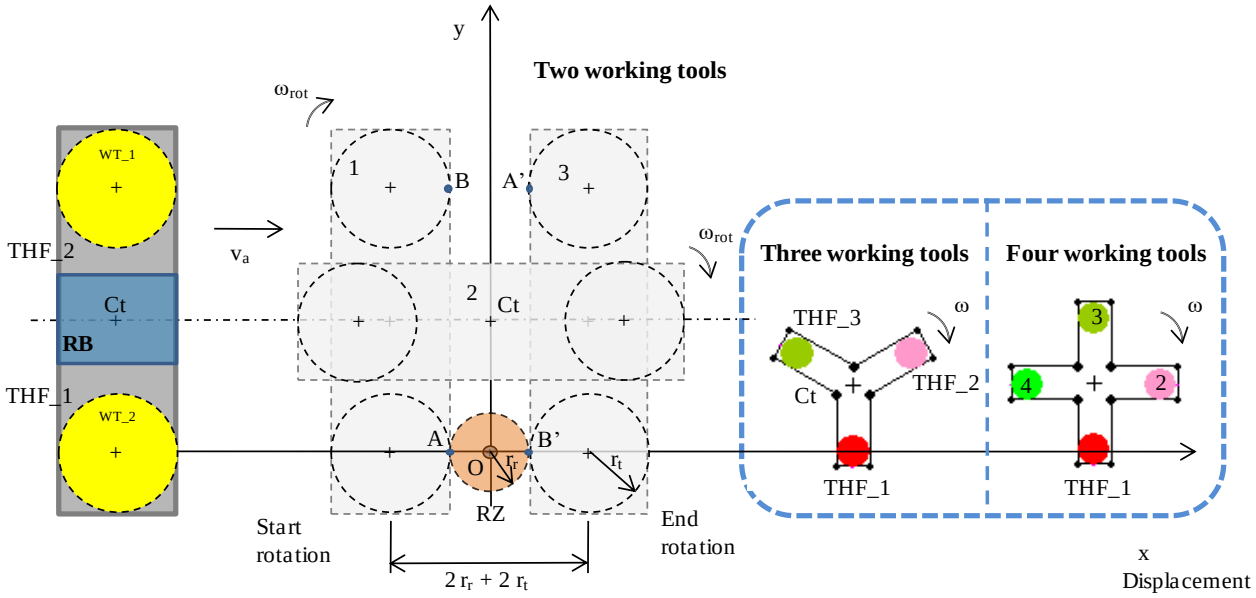

Figure 3: Sketch of the RPSS models with two THFs. This sketch is valid both for vertical and horizontal models (RPSS-VA, RPSS-HA). For the RPSS-VA model, the sketch represents the top view (the XY plane is parallel to the ground), while for the RPSS-HA model, the sketch is to be seen as a side view (the XY plane is perpendicular to the ground). In both models the x-axis represents the planted row. The framed figure on the right shows a simplification of configurations with three and four THFs.

ISSN: 2455-6939

Volume:05, Issue:01 "January-February 2019"

If we do not want to work outside the planted row (that is to work only in the intra-row) with the RPSS-VA model, it is possible to tilt the rotating axis of the RB towards the worked row by a suitable angle (Fig. 4). In this way only the WT on the row will be active, while the other one will be out of the ground.

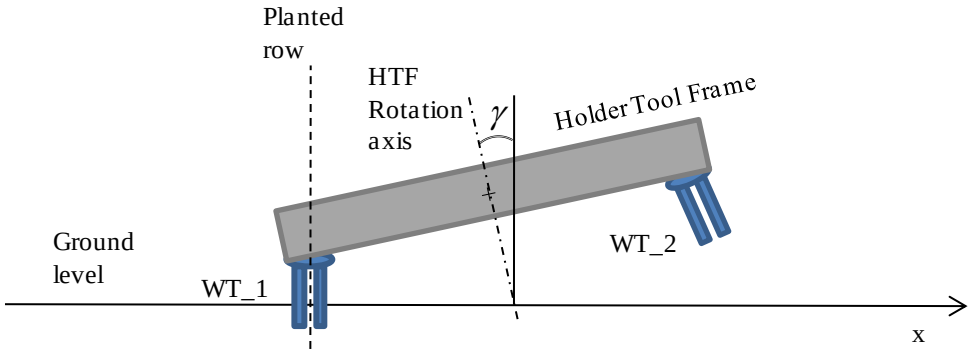

Figure 4: Side view of the RPSS-VA model with tilted rotation axis to enable to work only the WT in the row (WT_1), while WT_2 is away from the ground.

2.2.2. Forward-backward tilting plant-skipping system (FBTS)

In this model the RB has only one THF, and the rotation motion is not just in one direction, but it has a tilting rotation motion: in one direction of rotation the THF enters the row (at the angular speed of ω_R), in the opposite direction it exits the row (at the angular speed of ω_O, Fig. 5). As in the previous model, during its operation the THF is perpendicular to the row. The plant-skipping procedure follows three phases (Fig. 5):

1) Rotation of the THF (turning on the C pivot, Fig. A.1) in the sense of advancing of an angle of α_{max} at the given rotation speed of ω_O; rotation starts in C_{SX} and continues until the action area of the WT (with the action radius of r_t) is out of the RZ, that is in C_{EX} (Figures 5 and A.1); at this point the centre of WT is in the E_x point (Fig. 5));
2) The THF, fixed in the angular position reached at the previous step, by translation at the advancing speed v_a, skips the plant (in this phase the final point SR, reached by the centre of WT, is distinct for the FBTS-CR and the FBTS-VR models);
3) The THF enters again the row thanks to a rotation of an angle of α_{max} in the opposite direction of the phase 1. The starting point of rotation to enter the row begins at C_{SR} point in Fig. 5 and Fig. A.1, and the angular speed (ω_R) depends on the modality of the rotation, which can be constant (in the FBTS-CR model) or variable (in the FBTS-VR model, with controlled variable ω_R).

ISSN: 2455-6939

Volume:05, Issue:01 "January-February 2019"

Appendix A shows a detailed calculation of C_{SX}, C_{EX}, and α_{max}.

a) Return in the row at constant ω_R (FBTS-CR model)

In this case the translation (without rotation, with the THF fixed at α_{max}) of phase 2 of the plant-skipping procedure will continue up to the WT centre (C_{WT}, Fig. A.1) will pass the RZ in C_{SR} position with C_{SR} = + r_r as in Fig. 5b. At this point the return rotation at ω_{RCR} angular speed begins. Considering that the rotation of α_{max} will require the same time necessary to run the distance r_t to be completed, we can calculate ω_{RCR} as follows:

$$\omega_{R_{CR}} = \frac{v_a \cdot \alpha_{\max}}{r_t} \qquad (7)$$

b) Return in the row at controlled speed rotation ω_R (FBTS-VR model)

In this configuration the speed of rotation is controlled with the aim to follow as close as possible the RZ edge. Appendix B presents the Calculation of the starting point of rotation to return in the row (CSR) for the FBTS-VR model. The speed rotation of the THF is regulated by the following simple algorithm at each time step *dt*, after setting $\alpha = \alpha_{max}$:

$\alpha = \alpha - dt \cdot \omega_{R_{VR}}$;

If Distance (K, plant position) $\geq r_r$ *then* $\omega = \omega_{R_{VR}}$

else $\omega = 0$; // no rotation, only translation

ISSN: 2455-6939

Volume:05, Issue:01 "January-February 2019"

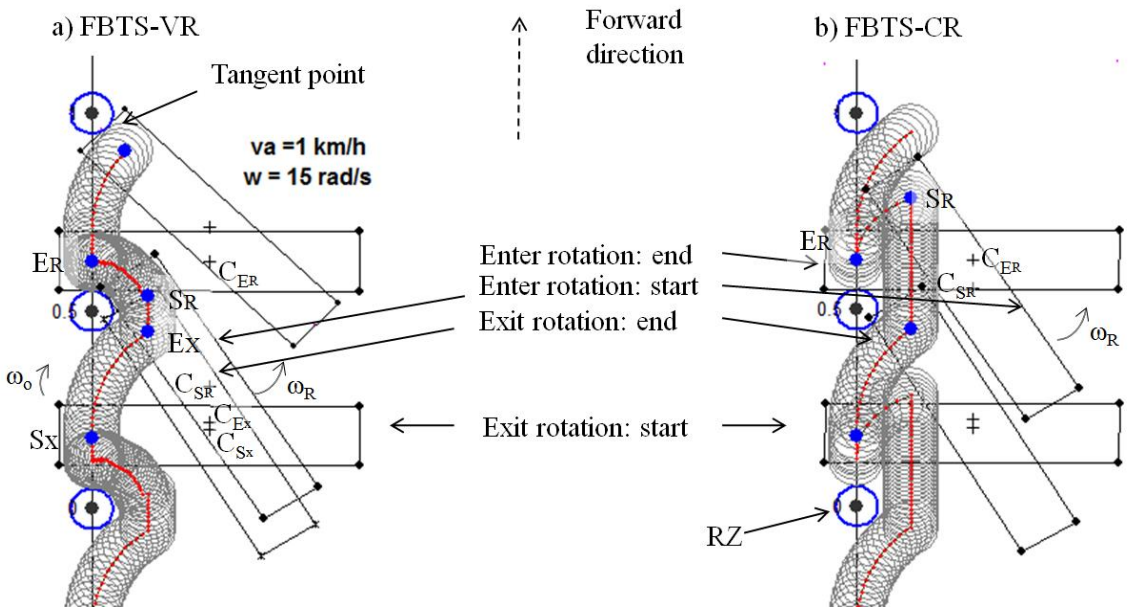

Figure 5: Model simulation of the Forward-backward tilting system (FBTS). a) at variable return angular speed (FBTS-VR); b) at constant return angular speed (FBTS-CR). Sx = start exit rotation, Ex = end exit rotation; S_R = start return rotation, E_R end return; C = centre of rotation of the THF. Red line = trajectory of the WT centre.

In this way the entering rotation of the THF proceeds in an irregular way until $\alpha = 0$ (Fig. 5.a).

The angular speed ω_{RVR} used is calculated considering that in the meantime that THF moves from C_{SR} to C_{ER} (just in the position outside the RZ), the THF performs the α_{max} rotation. Therefore, ω_{RVR} will be:

$$\omega_{R_{VR}} = \frac{v_a \cdot \alpha_{\max}}{(C_{SR} + C_{ER})} \qquad (8)$$

It is not possible to return in the row with a continuous rotation at ω_{RVR} since, if the final position remains the same of the controlled approach, the WT will invade the RZ.

The plant-skipping procedure could be done also by reversing the direction of the rotation to entering/exiting the row as described so far.

2.2.3. Rotary motion plant-skipping system - horizontal rotation axis (RPSS-HA model)

ISSN: 2455-6939

Volume:05, Issue:01 "January-February 2019"

This solution is similar to the *RPSS-VA*, but the rotation axis of the THF is horizontal and perpendicular to the row. So, the plant-skipping system is just similar to a wheel with two, three or four "spokes" (obviously, without the rim), each one is provided with a WT.

The angular speed of rotation of the "wheel" (ω_{rot}) is the same as in the *RPSS-VA* (Eqn. 6).

While rotating over the ground to skip the plant, in order to prevent the THF from hitting the plant itself during its movement, a suitable distance between two plants in the row must be ensured. As a reference the same scheme of Fig. 3 (used for the *RPSS-HA* model) can be used, but, in this case it has to be considered as a side view, differently from the *RPSS-HA* model, used as top view.

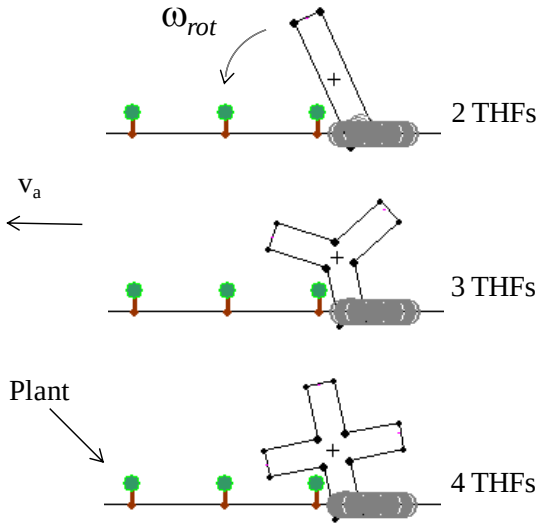

Figure 6: Side view of the rotary motion plant-skipping system with horizontal rotation axis *(RPSS-HA)*; solution with two, three, and four THFs (that is with two, three, and four WTs).

In general, for each given v_a and ω_{rot}, a minimum distance between the plants must be, depending also on the THF dimension (the radius of rotation *R*, and the width of the THF, that is *2* r_t). Referring to Fig. 7, it is possible to calculate the minimum distance between the plants in the row ($D_{t\,min}$), which is necessary to avoid damaging the plant during the rotation of the THF:

$$D_{t\,min} = \left| x_{A\,max} \right| + r_t + 2r_r \qquad (9)$$

ISSN: 2455-6939

Volume:05, Issue:01 "January-February 2019"

If ω_{rot} is calculated using Eqn. 6), $D_{t\,min}$ can be considered as an invariant with respect to v_a , on equal terms, because the angular position of the THF (α_{min}) inside the row (Fig. 7) is always the same.

Appendix C contains a detailed calculation of $x_{A\,max}$ and α_{min}.

For this model the working parameters can be analytically calculated as follows:

$$\left.\begin{array}{l} 1.RWA = [D - 2\,(r_r + r_t)]\,2\,r_t + \pi\,r_t^{\,2} \\ 4.WR = D - 2\,r_t \\ 4.1.WR = 100\% \end{array}\right\} \quad (10)$$

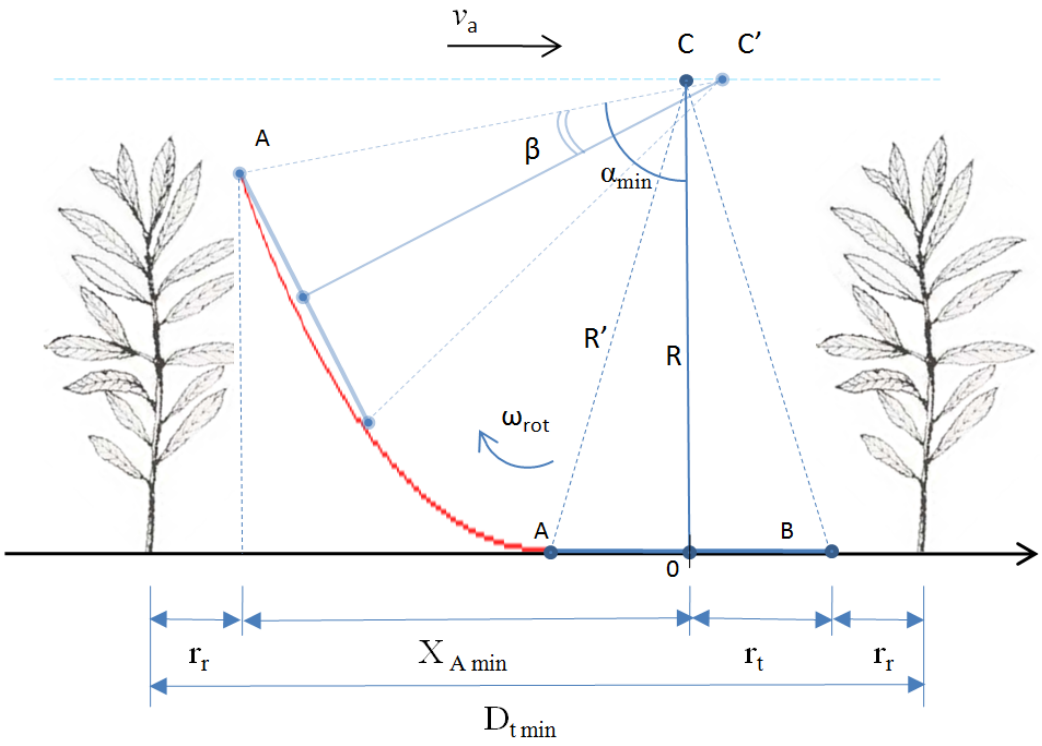

Figure 7: Sketch used to calculate the minimum distance between two plants in the row ($D_{t\,min}$). The AB segment represents the diameter of the WT, while R is the radius of the THF. C-C' = THF advancement during α_{min} rotation.

3. RESULTS AND DISCUSSION

In order to make a suitable comparison among the different models proposed in the present paper, all the simulations were performed using the following settings:

- Radius of the working tool: r_t = 0.075 m;
- Radius of the Respect zone: r_r = 0.05 m;
- Radius of the THF: R = 0.35 m. In the *RPSS* models, the radius depends on the number of THFs used (2, 3, or 4); the selected radius is the one that allows for the maximum worked area around the RZ;
- Row spacing: D = 0.5 m (slightly greater than that required by the *RPSS-HA* model: $D_{t\,min}$ = 0.41 m);
- Advancing velocity: v_a = 0.28, 0.56, and 0.83 m s^{-1} (respectively 1.0, 2.0, and 3.0 km h^{-1}). The selected velocities are those normally used with the most common weeding operating machines (both hydraulically- or mechanically-driven with rotating working tools).

Table 4: Results for the CDSS and RPSS models.

Test #	Plant-skipping system	# working tools	Advancing velocity (v_a, km/h)	Crossing velocity (v_r, km/h)	Body length (m)	1.RWA - Row centered strip worked area (m^2)	1.1.RWA% - Row centered worked area (%)	2.1. OWA% Worked area outside row strip (%)	2.2. OWAR% Outwards worked area in term of 1.RWA (%)	3.WWA - Width of the worked area (m)	4.1.WR% Worked row (%)	X_R (m)
1	Cross displacemet system (CDSS)	1	1.0	1.0	0.50	0.057	85.0	59.3	67.5	0.21	89.6	0.102
2		1	1.0	2.0	0.50	0.062	92.4	62.6	63.1	0.20	97.0	0.065
3		1	1.0	3.0	0.50	0.063	93.4	65.5	67.9	0.21	98.6	0.057
4		1	1.0	5.0	0.50	0.063	94.5	69.8	68.7	0.20	99.5	0.052
5		1	3.0	5.0	0.50	0.062	92.4	59.4	59.8	0.20	95.8	0.071
				Angular velocity, ω_{rot} (rad/s)	Radius of the rotating body (m)							
6	Rotary motion system Vertical axis (RPPS- VA) (*)	2	1.0	3.5	0.16	0.064	95.9	96.4	127.2	0.25	100.0	
7		3	1.0	2.3	0.20	0.063	93.9	89.9	178.3	0.33	100.0	
8		4	1.0	1.7	0.25	0.061	91.0	98.6	282.3	0.43	100.0	
9		2	2.0	7.0	0.16	0.064	95.9	96.2	127.0	0.25	100.0	
10		3	2.0	4.7	0.20	0.063	93.9	89.8	178.0	0.33	100.0	
11		4	2.0	3.5	0.25	0.061	91.1	98.6	282.0	0.43	100.0	
12		2	3.0	10.5	0.16	0.064	95.4	96.1	127.6	0.25	100.0	
13		3	3.0	7.0	0.20	0.063	93.6	88.9	177.0	0.33	100.0	
14		4	3.0	5.2	0.25	0.061	90.7	97.9	281.2	0.43	100.0	
15	Rotary motion system Horizontal axis (RPSS- HA) (*)	2-4	1.0 - 3.0	3.5 - 1.7	0.35	0.038	55.8	0.0	0.0	0.075	100.0	

(*) ω_{rot} calculated with Eqn. 6)
Row spacing, D = 0.50 m
Diameter of the working tool, 2 r_t = 0.15 m
Diameter of the respect zone, 2 r_r = 0.10 m

Tab. 4 shows the results for the CDSS and RPSS-VA and RPSS-HA models, while Tab. 5 lists the results for the FBTS-CR and FBTS-VR models coming from the simulation software. For the RPSS-HA the working parameters are drawn by analytical calculations, and not by simulation.

CDSS model

ISSN: 2455-6939

Volume:05, Issue:01 "January-February 2019"

In the CDSS model, with $v_r/v_a > 1.5$, there is no significant reduction in the distance X_R (the starting point to enter the row), as its derivative tends to zero (Fig. 8).

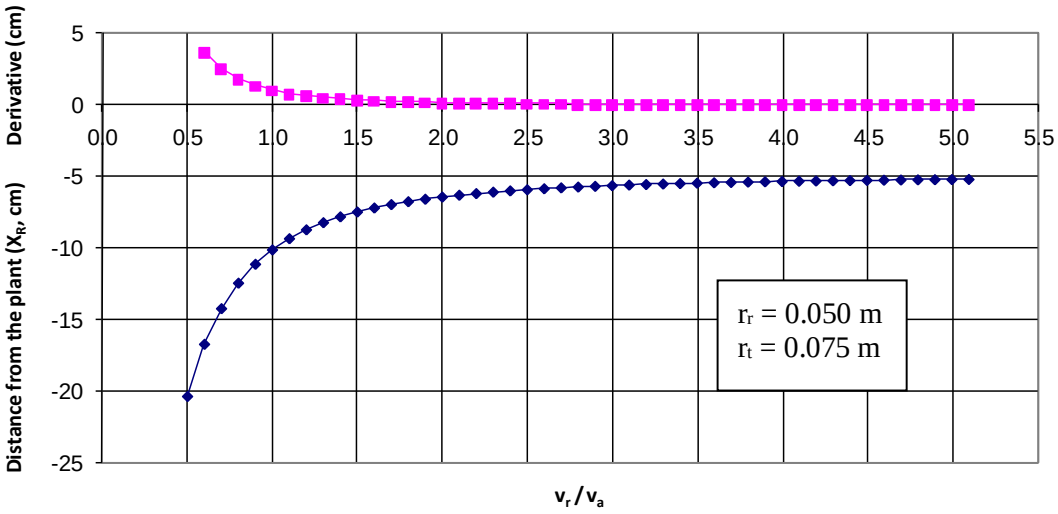

Figure 8: Entering distance (X_R) and its derivative with respect to v_r/v_a for the CDSS model.

Fig. 9 shows the trends for three different v_a/v_r ratios.

Tab. 4 explains how X_R decreases from 0.102 m (Test# 1), with v_a/v_r=1/1, to 0.065 m (Test# 2), with v_a/v_r = 1/2, but by passing to v_a/v_r = 1/3, X_R the reduction is only 0.008 m (Test# 3).

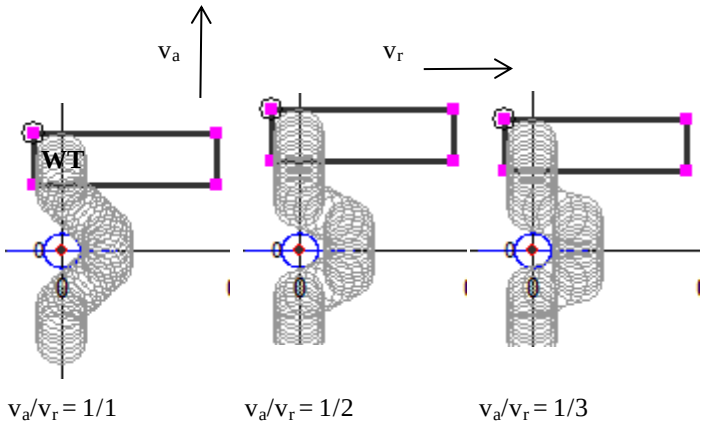

Figure 9: CDSS model: WT patterns with different v_a/v_r ratios (1/1, 1/2, and 1/3, respectively).

ISSN: 2455-6939

Volume:05, Issue:01 "January-February 2019"

RPSS-VA model

Fig. 10 presents the patterns of three configurations of the RPSS-VA model. In this case, if ω_{rot} is calculated using Eqn. 6), the patterns are the same for any v_a setting.

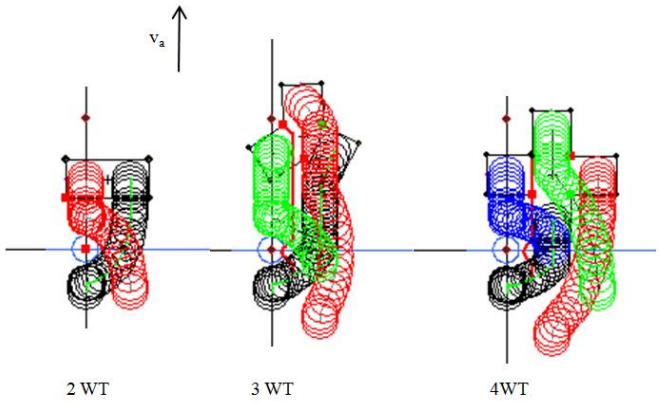

Figure 10: RPSS-VA models (top view): WT paths with different number of THFs.

Working parameters comparisons

Row centered strip worked area / Interested row centered area (%) - 1.1.RWA% index

Considering that the maximum workable area (*MWAR*) along the row is given by $MWAR = D\ 2r_t - \pi\ r_r^2$ (in this work = 0.067 m^2), we can make comparisons among the models by taking into account the percentage of the worked area (1.1.RWA%). This index, for the CDSS model, ranges from 58% up to 93.4% with a v_a/v_r ratio of 1/1 and 1/3, respectively. The same happens for the worked row (4.WR). The RPSS-VA with 2 THFs shows the best performance with 1.1.RWA% = 95.9 % (Test# 6).

The worst performance comes from the FBTS-CR model, with v_a = 0.83 m s^{-1} (3 km h^{-1}) and ω_{rot} = 10 rad s^{-1} (1.1.RWA% = 82.1%, Test# 21). The FRS-VR shows a similar behavior.

The rotative models (RPSS and FBTS) show the best performance with respect to the worked row (RZ excluded, the maximum WR is given by D - 2 r_r = 0.4 m). In particular the RPSS model gives the maximum worked row allowed (4.1.WR% = 100%, Tests# 6-15) for all the tested operative conditions, while in the FBTS models 4.1.WR% ranges from 96.3% (Test# 16, 17, etc.) up to 98.8% (Test# 26).

The FBTS models (CR and VR) with operative parameters set at v_a = 0.83 m s^{-1} and ω_{rot} = 5 rad s^{-1} are not able to sufficiently and conveniently exit the row, so the WT invades the RZ (4.1.WR% > 100%, Tests#18 and 27).

The performance of the CDSS model can be extremely good at low v_a/v_r ratio. With v_a/v_r = 1/3 the worked row is 4.1.WR% = 98.6% (Test#3).

Outwards worked area in term of row strip worked area (%) - 2.2.%OWARS index

The worked area outside the row by the CDSS model is at maximum 67.9%, with v_a = 0.83 m s^{-1} , and v_r = 0.28 m s^{-1} (1 km h^{-1}) (Tab. 4, Test#3), while the RPSS-VA models ranges from 127.2% to 282.3%, passing from 2 WTs to 4 WTs (Tests# 6-8 for v_a = 0.28 m s^{-1}; same results with any v_a, because ω_{rot} is calculated with Eqn. 6).

The FBTS-CR model ranges from 92% to 112.1%, while the FBTS-VR model shows values comparable with the CDSS model, with a percentage of worked area going from 57.5% (Tab. 5, Test# 27, the absolute minimum) to 71.3% (Test# 33).

Table 5: Results for the FBTS-CR and FBTS-VR models.

Test #	Plant-skipping system	Advancing velocity (v_a, km/h)	Outward angular velocity, ω_O (rad/s)	Return angular velocity, ω_R (rad/s)	1.RWA - Row centered strip worked area (m^2)	1.1.RWA% - Row centered worked area (%)	2.1. OWA% Worked area outside row strip (%)	2.2.OWAR% Outwards worked area in term of 1.RWA (%)	3.WWA - Width of the worked area (m)	4.1.WR% Worked row (%)
				Constant						
16	Forward-backward balancing system ω_{return} = constant (FBTS-CR)	1.0	5.00	3.68	0.056	83.3	97.0	108.4	0.20	96.3
17		2.0	5.00	7.36	0.055	82.6	95.4	107.4	0.20	96.3
18		3.0	5.00	11.04	0.060	89.8	88.8	92.0	0.20	110.0
19		1.0	10.00	3.68	0.057	84.2	97.1	107.3	0.20	96.3
20		2.0	10.00	7.36	0.056	83.6	97.1	108.1	0.20	97.5
21		3.0	10.00	11.04	0.055	82.1	96.5	109.4	0.20	95.0
22		1.0	15.00	3.68	0.057	84.5	96.5	110.5	0.21	97.5
23		2.0	15.00	7.36	0.057	84.6	96.1	110.0	0.21	97.5
24		3.0	15.00	11.04	0.056	82.9	96.0	112.1	0.21	96.3
				Variable (controlled)						
25	Forward-backward balancing system ω_{return} = variable (FBTS-VR)	1.0	5.00	0.89	0.056	84.0	64.3	71.2	0.20	96.3
26		2.0	5.00	1.80	0.057	84.5	62.5	68.8	0.20	98.8
27		3.0	5.00	2.77	0.060	89.1	55.1	57.5	0.20	107.5
28		1.0	10.00	0.88	0.057	85.4	63.3	69.0	0.20	97.5
29		2.0	10.00	1.81	0.056	84.0	63.8	70.7	0.20	96.3
30		3.0	10.00	2.76	0.056	83.8	63.2	70.2	0.20	96.3
31		1.0	15.00	0.89	0.057	85.6	61.6	69.6	0.21	97.5
32		2.0	15.00	1.81	0.057	84.8	61.7	70.5	0.21	96.3
33		3.0	15.00	2.80	0.057	84.2	62.0	71.3	0.21	96.3

Row spacing, D = 0.50 m
Diameter of the working tool, 2 r_t = 0.15 m
Diameter of the respect zone, 2 r_r = 0.10 m

ISSN: 2455-6939

Volume:05, Issue:01 "January-February 2019"

In relation to the need to work or not out of the row strip (*2.1.OWA* and *2.1.%OWARS* indexes), or how much to work, these model simulations represent a help to choose the best solution for a specific task. So, for example, if we do not want to work out of the row, the best solution is represented by the RPSS-HA models (2.1.%OWARS = 0.0%); alternatively, among the models with vertical rotation axis (RPSS-HA), the minimum external worked area is obtained with 2 WTs (a higher number of WTs gives a higher *2.1.%OWARS* index).

Among the different tilting systems (FBTS models) the FBTS-VR model gives the lowest *2.1.%OWARS* index (at maximum 71.3%, Test# 33).

The main cause of soil irregularity during working (formation of depressions and dunes) is due to the displacement of the WT. So, to limit this problem, we can opt for the RPSS-VA model with 3 or 4 WTs, since, at equal working speed, a higher number of WTs allows for a reduction in relative displacement, and, consequently, slighter soil profile modifications.

The total width of the worked area is another important aspect to improve weed control. To reduce the non-worked area, we need to increase the number of WTs using 3 or 4 WTs with the RPSS-VA model. In this case we have a 3.WWA index of 0.43 m with 4 WTs, while with only 2 WTs we have just 0.25 m.

4. APPLICATION NOTES

In all the proposed models it is possible to use a stepping motor to better control the rotation (in RPSS models) or the partial clockwise and counter clockwise rotation (in FBTS models).

4.1. Configurations without control unit

RPSSs do not need a control unit to be operative in a weeding machine. In order for it to correctly work as described in paragraph 2.1, it must be equipped with a sensor (see Assirelli et al., 2015) to detect in advance the plant at a distance r_r from the point A of the THF (Fig. 3), to give the command to start the rotation of the THF itself. In order to skip the plant without damaging it, ω_{rot} must be set by considering Eqn. 6. If we consider to operate the THF by means of a free wheel with a radius R_{FW}, and an angular velocity ω_{FW}, ($\omega_{FW} = v_a / R_{FW}$), the transmission ratio TR can be calculated as follows:

$$TR = \frac{\omega_{rot}}{\omega_{FW}} = \frac{R_{FW} \cdot \pi}{n_{WT} \cdot (r_r + r_t)} \qquad (11)$$

4.2. Configurations using a control unit

ISSN: 2455-6939

Volume:05, Issue:01 "January-February 2019"

While a control unit is not necessary in RPSSs, it is essential in FBTSs, in order to guide the partial rotations to enter and exit the row. The control unit becomes absolutely necessary with the FBTS-VR to continuously regulate the angular speed during the entering rotation, with regard to the advancing speed v_a. In this case a stepping motor should be used in order to operate the THF and enable an accurate adjustment of the rotation.

5. CONCLUSIONS

Working machines for intra-row weed control can differ according to their constructional and functional typology, as well as according to the function of the different working depths. The availability of a simulation model to evaluate in advance their performances can help the machine manufacturer to design and develop new solutions, also by taking into account a given planting layout. The construction typology directly influences also the kinematic chain and the overall complexity of the identified working system. Different types of driving power can provide for different solutions, going from the mechanical to the hydraulic power, to the electric power, mainly depending on the required power level. Most modern tractors show enough potential in all these modalities. Even the electric drive would not require significant integrations in most of the available electrical systems.

The present theoretical study has shown new systems to perform the mechanical weed control within the planted row. The main idea focuses on the use of a rotating system (rotating, RPSS, or partially rotating, i.e. tilting, FBTS) to skip the plant of the crop to be left, in opposition to the traditional crosswise translation one (CDSS).

The different configurations experimented by means of simulation models have produced different results: the RPSS-HA allows to work only in the row (intra-stool space), while all the other models present also a worked area outside the row.

In the proposed models it is possible to use a stepping motor in order to continuously adjust the speed of rotation as a function of the working speed. In particular, for the FBTS-VR model, due to the continuous control of the rotation during row entering, such motor becomes key.

On the contrary, a free wheel with a suitable transmission ratio is sufficient to power RPSSs.

This work aims to provide a guidance to construction and functional modalities, as well as mechanisms, to apply to weed control, with the main scope of limiting the environmental impact of technology, in full respect of the concepts of a sustainable and precision agriculture. Further model implementations, including aspects related to soil typology, could allow for a more accurate assessment of the suitability of tools of different shapes, configurations, functional

working principles in relation to the actual cultivation conditions (e.g. level of growing, etc.), and also of different pedoclimatic conditions. Such considerations would play a very important role in reducing soil organic matter content, often attributed to a strong impact of mechanical actions (e.g. considerable working depth), or to wrong weeding with respect to crop growth.

Finally, another aspect that can be drawn from the present work, and that does not concern directly weed control, is the possibility to eliminate the surface crust with positive effects on water management and gaseous soil exchanges, especially in the nursery and in those areas directly affected by the roots of young plants. In this case the RPSS-VA approach allows to obtain the highest worked area outside the row (in the inter-row space).

The work was supported by the AGROENER project (D.D. no. 26329, 1 April 2016, *http://agroener.crea.gov.it/*) through funding granted from the MinisterodellePolitiche Agricole Alimentari, Forestalie del Turismo (MIPAAFT).

REFERENCES

Assirelli, A., Liberati, P., Santangelo, E., Del Giudice, A., Civitarese, V., Pari, L., Evaluation of sensors for poplar cutting detection to be used in intra-row weed control machine. (2015) Computers and Electronics in Agriculture, 115, pp. 161-170. DOI: 10.1016/j.compag.2015.06.001.

Davies, D.H.K., Hoad, S., Maskell, P.R., Topp, K. 2004 Looking at cereal varieties to help reduce weed control inputs. Proceedings Crop Protection in Nothern Britain

Gaines, T. A., W. Zhang, D. Wang, B. Bukuna, S. T. Chisholm, D. L. Shaner, S. J. Nissen, W. L. Patzoldt, P. J. Tranel, A. S. Culpepper, T. L. Grey, T. M. Webster, W. K. Vencill, R. D. Sammons, J. Jiang, C. Preston, J. E. Leach, and P. Westra. 2010. Gene amplification confers glyphosate resistance in Amaranthus palmeri. Proc. Natl. Acad. Sci. 107:1029–1034. CrossRef, PubMed.

Hoad, S., Topp, C., Davies, K. 2008 Selection of cereals for weed suppression in organic agriculture: a method based on cultivar sensitivity to weed growth. Euphytica. vol.163: 355-366

ISTAT 6°Censimento Generale Agricoltura, 2013, Pagine: 428, ISBN: 978-88-458-1777-9 (stampa), ISBN: 978-88-458-1779-3.

Li Nan, Zhang Chunlong , Chen Ziwen, Ma Zenghong, Sun Zhe, Yuan Ting, Li Wei, Zhang Junxiong. 2015. Crop positioning for robotic intra-row weeding based on machine vision. Int J Agric & Biol Eng. Vol. 8 No.6: 20-29.

Perez-Jones, A., K. W. Park, J. Colquhoun, C. A. Mallory-Smith, and D. Shaner. 2005. Identification of glyphosate-resistant Italian ryegrass (Lolium multiflorum) in Oregon. Weed Sci. 53:775–779. BioOne

Pérez-Ruíz M., Slaughter D.C., Fathallah F.A., Gliever C.J., Miller B.J. 2014. Co-robotic intra-row weed control system. Biosyst. Eng. 126:45-55. http://dx.doi.org/10.1016/j.biosystemseng.2014.07.009.

Peruzzi, A., Martelloni, L., Frasconi, C., Fontanelli, M., Pirchio, M., & Raffaelli, M. (2017). Machines for non-chemical intra-row weed control in narrow and wide-row crops: a review. Journal Of Agricultural Engineering, 48(2), 57-70. doi: http://dx.doi.org/10.4081/jae.2017.583.

Rasmussen J., Griepentrog H.W., Nielsen J., Henriksen C.B. 2012. Automated intelligent rotor tine cultivation and punch planting to improve the selectivity of mechanical intra-row weed control. Weed Res. 52:327-37. DOI: 10.1111/j.1365-3180.2012.00922.x

Rueda-Ayala V., Peteinatos G., Gerhards R., Andújar D. 2015. A non-chemical system for online weed control. Sensors 2015, 15, 7691-7707; doi:10.3390/s150407691

Salas, R. A., F. E. Dayan, Z. Pan, S. B. Watson, J. W. Dickson, R. C. Scott, and N. R. Burgos. 2012. EPSPS gene amplification in glyphosate-resistant Italian ryegrass (Lolium perenne ssp. multiflorum) from Arkansas. Pest Manag. Sci. 68:1223–1230. CrossRef, PubMed

Van der Weide R.Y., Bleeker P.O., Achten V.T.J.M., Lotz L.A.P., Fogelberg F., Melander B. 2008. Innovation in mechanical weed control in crop rows. Weed Res. 48:215-24. DOI: 10.1111/j.1365-3180.2008.00629.x

ISSN: 2455-6939

Volume:05, Issue:01 "January-February 2019"

Appendix A

Calculation of C_{SX}, C_{EX}, and α_{max}

Calculation of the starting point of rotation to exit the row (C_{SX})
The trajectory of the outsider point of the THF (point B, Fig. A.1), a cycloid function, is described by the following parametric functions:

$$x_B = C_{SX} + t \cdot v_a + R \cdot \sin(\omega \cdot t) \qquad (A.1)$$

$$y_B = Y_{IR} - R \cdot [1 - \cos(\omega \cdot t)] \qquad (A.2)$$

Where

C_{SX} = the x-coordinate of the RB centre in which the rotation starts skipping the plant; the condition to calculate C_{SX} is given by the tangency of the cycloid with the ZR circle.

Y_{IR} = sets how much the WT enters the row. In this work Y_{IR} = - r_t (the radius of the working tool)

R = overall rotation radius of the THF (Fig. A.1).

Starting from C_{SX}, the THF rotates by α_{max} to reach a position where the WT does not affect the RZ.

After a rotation of an angle of α_{tan} ($\alpha_{tan} > \alpha_{max}$), in a time t_{tan}, the point B of the cycloid will be tangent to the RZ circle (Fig. A.1). In the meantime the C_{SX} point advances by a distance of $v_a \cdot t_{tan}$.

Referring to the triangle OCT, α_{tan} can be calculated by the following equation:

$$\alpha_{\tan} = a\cos\left(\frac{R - r_t}{R + r_r}\right) \qquad (A.3)$$

While t_{tan} will be

$$t_{\tan} = \frac{\omega_o}{\alpha_{\tan}} \qquad (A.4)$$

ISSN: 2455-6939

Volume:05, Issue:01 "January-February 2019"

Angular speed ω_O is not calculated, but it is given, depending on design needs. The abscissa of the C_{SXT}, the centre of the THF when B point is tangent to the RZ (T in Fig. A.1), is given by $T = -(R + r_r) \sin(\alpha_{tan})$; the starting point of rotation as in step 1 is in C_{SX}, that is backwards with respect to T by $v_a \cdot t_{tan}$. So the abscissa where the rotation starts skipping the plant will be:

$$C_{SX} = -\left[(R + r_r) \cdot \sin(\alpha_{\tan}) + v_a \cdot t_{\tan}\right] \qquad (A.5)$$

Calculation of the ending point of rotation to exit the row(C_{EX})

The rotation will end when the circle of WT is just outsidethe RZ as y-coordinate (the centre of C_t is in the C_{EX} position in Fig. A.1). The condition to save the RZ is given by the following:

$$r_r + r_t = -\left[R + r_r \cdot \cos(\alpha_{\tan})\right] \qquad (A.6)$$

From which we obtain

$$\alpha_{\max} = a\cos\left(-\frac{r_r + 2r_t}{R}\right) \qquad (A.7)$$

And

$$t_{\max} = \frac{\omega_o}{\alpha_{\max}} \qquad (A.8)$$

Therefore C_{EX} will be:

$$C_{EX} = C_{SX} + v_a \cdot t_{\max} \qquad (A.9)$$

The angle α_{max} depends only on dimensional parameters (R, r_r, and r_t,), while C_{SX} depends also

ISSN: 2455-6939

Volume:05, Issue:01 "January-February 2019"

on v_a and ω_O.

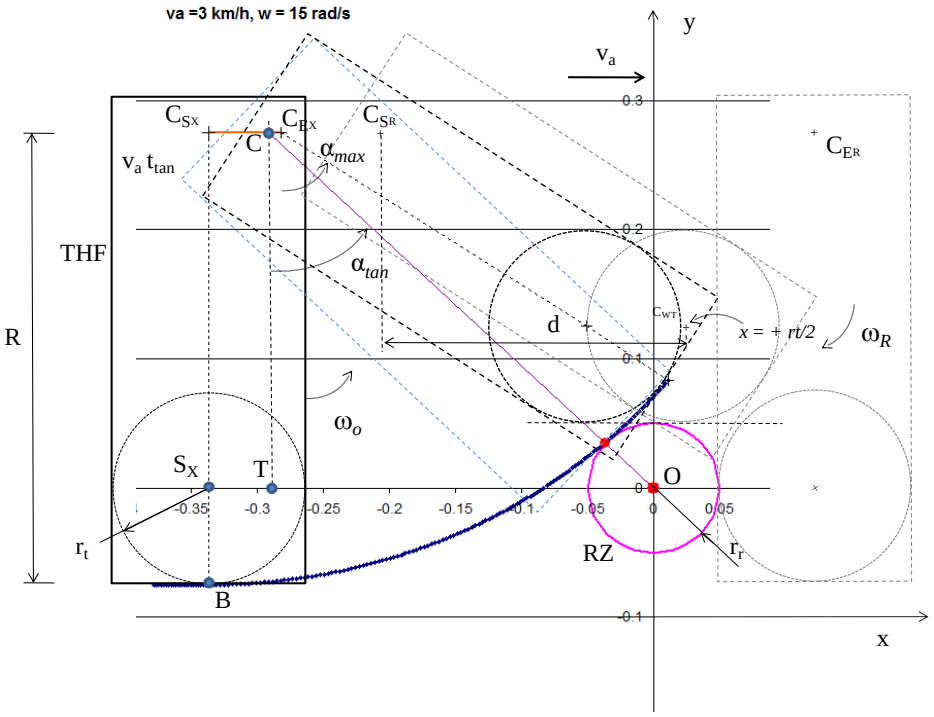

Figure A.1: Sketch used to calculate the start/end rotation position to exit/enter the row (SX, EX, SR, ER) for the FBTS-CR model.

Appendix B

Calculation of the starting point (C_{SR}) of rotation to return in the row for FBTS-VR model

Considering that translation goes from point C_{EX} to point C_{SR}, which corresponds to the position of C_{WT} at $+r_t/2$ with respect to Fig. A.1, C_{SR} can be calculated as:

$$C_{SR} = +\frac{r_r}{2} - d \qquad (B.1)$$

Where

$$d = (R - r_r) \cdot \sin(\alpha_{max}) \qquad (B.2)$$

Appendix C

ISSN: 2455-6939

Volume:05, Issue:01 "January-February 2019"

Calculation of $x_{A\,min}$ and α_{min} for RPSS-HA model

Referring to Fig. 7, and taking into account the composed motion of rotation and translation, the coordinates of the point A as a function of time is given by the following parametric equations:

$$y_A = R - R' \cdot \cos\left(\omega t + \beta\right) \qquad (C.1)$$

$$x_A = v_a \cdot t - R' \cdot \sin\left(\omega t + \beta\right) \qquad (C.2)$$

Where β is calculated as follows:

$$\beta = \arctan\left(\frac{r_t}{R}\right) \qquad (C.3)$$

And R' as:

$$R' = \sqrt{R^2 + r_t^2} \qquad (C.4)$$

By setting to zero the derivative of Eqn. C.2), it is possible to obtain the time t_{min}, that is to say the time needed by A (Fig. 7) to reach the minimum value $x_{A\,min}$ (the maximum distance if considered in absolute terms):

$$t_{\min} = \frac{1}{\omega_{rot}}\left[\arccos\left(\frac{v_a}{\omega_{rot} R'}\right) - \beta\right] \qquad (C.5)$$

To obtain $x_{A\,min}$ we can replace β and t_{min} into Eqn C.2) with Eqn C.3) and Eqn C.5), respectively:

$$x_{A\min} = \frac{v_a}{\omega_{rot}}\left[\arccos\left(\frac{v_a}{\omega_{rot} R'}\right) - \arctan\left(\frac{r_t}{R}\right)\right] - R' \cdot \sin\left(\arccos\left(\frac{v_a}{\omega_{rot} R'}\right)\right) \qquad (C.6)$$

The angular position of the THF at $x_{A\,min}$ is given by the following equation:

$$\alpha_{\min} = \omega_{rot} \cdot t_{\min} = \arccos\left(\frac{v_a}{\omega_{rot} R'}\right) - \beta \qquad (C.7)$$

